Received 11 April 2001; accepted 1 July 2002; doi:10.1038/nature00952.

1. Hagfeldt, A. & Grätzel, M. Molecular photovoltaics. *Acc. Chem. Res.* **33,** 269–277 (2000).
2. Vlček, A. Jr The life and times of excited states of organometallic and coordination compounds. *Coord. Chem. Rev.* **200–202,** 933–977 (2000).
3. Grätzel, M. Photoelectrochemical cells. *Nature* **414,** 338–344 (2001).
4. Miller, R. J. D., McLendon, G. L., Nozik, A. J., Schmickler, W. & Willig, F. *Surface Electron Transfer Processes* (VCH Publishers, New York, 1995).
5. Tachibana, Y., Moser, J. E., Grätzel, M., Klug, D. R. & Durrant, J. R. Subpicosecond interfacial charge separation in dye-sensitized nanocrystalline titanium dioxide films. *J. Phys. Chem.* **100,** 20056–20062 (1996).
6. Hannappel, T., Burfeindt, B., Storck, W. & Willig, F. Measurement of ultrafast photoinduced electron transfer from chemically anchored Ru-dye molecules into empty electronic states in a colloidal anatase TiO_2 film. *J. Phys. Chem. B* **101,** 6799–6802 (1997).
7. Asbury, J. B., Hao, E., Wang, Y., Ghosh, H. N. & Lian, T. Ultrafast electron transfer dynamics from molecular adsorbates to semiconductor nanocrystalline thin films. *J. Phys. Chem. B* **105,** 4545–4557 (2001).
8. Heimer, T. A., Heilweil, E. J., Bignozzi, C. A. & Meyer, G. J. Electron injection, recombination, and halide oxidation dynamics at dye-sensitized metal oxide interfaces. *J. Phys. Chem. A* **104,** 4256–4262 (2000).
9. Benkö, G., Kallioinen, J., Korppi-Tommola, J. E. I., Yartsev, A. P. & Sundström, V. Photoinduced ultrafast dye-to semiconductor electron injection from nonthermalized and thermalized donor states. *J. Am. Chem. Soc.* **124,** 489–493 (2002).
10. Yeh, A. T., Shank, C. V. & McCusker, J. K. Ultrafast electron localization dynamics following photo-induced charge transfer. *Science* **289,** 935–938 (2000).
11. Tachibana, Y., Haque, S. A., Mercer, I. P., Durrant, J. R. & Klug, D. R. Electron injection and recombination in dye sensitized nanocrystalline titanium dioxide films: A comparison of ruthenium bipyridyl and porphyrin sensitizer dyes. *J. Phys. Chem. B* **104,** 1198–1205 (2000).
12. Damrauer, N. H. *et al.* Femtosecond dynamics of excited-state evolution in $[Ru(bpy)_3]^{2+}$. *Science* **275,** 54–57 (1997).
13. Blanchet, V., Zgierski, M. Z., Seideman, T. & Stolow, A. Discerning vibronic molecular dynamics using time-resolved photoelectron spectroscopy. *Nature* **401,** 52–54 (1999).
14. Willig, F., Zimmermann, C., Ramakrishna, S. & Storck, W. Ultrafast dynamics of light-induced electron injection from a molecular donor into the wide conduction band of a semiconductor as acceptor. *Electrochim. Acta* **45,** 4565–4575 (2000).
15. Wurth, W. & Menzel, D. Ultrafast electron dynamics at surfaces probed by resonant Auger spectroscopy. *Chem. Phys.* **251,** 141–149 (2000).
16. Brühwiler, P. A., Karis, O. & Mårtensson, N. Charge transfer dynamics studied using resonant core spectroscopies. *Rev. Mod. Phys.* **74,** 703–740 (2002).
17. Lanzafame, J. M., Palese, S., Wang, D., Miller, R. J. D. & Muenter, A. A. Ultrafast nonlinear optical studies of surface reaction dynamics: Mapping the electron trajectory. *J. Phys. Chem.* **98,** 11020–11033 (1994).
18. Nazeeruddin, M. K. *et al.* Conversion of light to electricity by cis-X_2bis(2,2′-bipyridyl-4,4′-dicarboxylate)ruthenium(II) charge transfer sensitizers ($X = Cl^-$, Br^-, I^-, CN^-, and SCN^-) on nanocrystalline TiO_2 electrodes. *J. Am. Chem. Soc.* **115,** 6382–6390 (1993).
19. Rensmo, H. *et al.* XPS studies of Ru-polypyridine complexes for solar cell applications. *J. Chem. Phys.* **111,** 2744–2750 (1999).
20. Patthey, L. *et al.* Adsorption of bi-isonicotinic acid on rutile TiO_2(110). *J. Chem. Phys.* **110,** 5913–5918 (1999).
21. Persson, P. & Lunell, S. Binding of bi-isonicotinic acid to anatase TiO_2(101). *Solar Energy Mater. Solar Cells* **63,** 139–148 (2000).
22. Cronemeyer, D. C. Electrical and optical properties of rutile single crystals. *Phys. Rev.* **87,** 876–886 (1952).
23. O'Regan, B. & Grätzel, M. A low-cost, high-efficiency solar cell based on dye-sensitized colloidal TiO_2 films. *Nature* **353,** 737–740 (1991).
24. Persson, P. *et al.* N 1*s* x-ray absorption study of the bonding interaction of bi-isonicotinic acid adsorbed on rutile TiO_2(110). *J. Chem. Phys.* **112,** 3945–3948 (2000).
25. Chang, E. K., Rohlfing, M. & Louie, S. G. Excitons and optical properties of alpha-quartz. *Phys. Rev. Lett.* **85,** 2613–2616 (2000).
26. Sandell, A. *et al.* Bonding of an isolated K atom to a surface: Experiment and theory. *Phys. Rev. Lett.* **78,** 4994–4997 (1997).
27. Lu, H., Prieskorn, J. N. & Hupp, J. T. Fast interfacial electron transfer: Evidence for inverted region kinetic behavior. *J. Am. Chem. Soc.* **115,** 4927–4928 (1993).
28. Ramakrishna, S. & Willig, F. Pump-probe spectroscopy of ultrafast electron injection from the excited state of an anchored chromophere to a semiconductor surface in UHV: A theoretical model. *J. Phys. Chem. B* **104,** 68–77 (2000).
29. Petersson, Å., Ratner, M. & Karlsson, H. O. Injection time in the metal oxide-molecule interface calculated within the tight-binding model. *J. Phys. Chem. B* **104,** 8498–8502 (2000).

Supplementary Information accompanies the paper on *Nature*'s website (http://www.nature.com/nature).

Acknowledgements

We are grateful for financial support to the Consortium on Clusters and Ultrafine Particles and to the ATOMICS Consortium, which are funded by Stiftelsen for Strategisk Forskning, to Göran Gustafssons Stiftelse, and to Vetenskapsrådet. We acknowledge the Swedish National Supercomputer Centre (NSC) for computer time, and the Group for Numerically-intensive Computations of the IBM Research Laboratory Zürich and the Abteilung Parrinello of MPI Stuttgart for help with the calculations.

Competing interests statement

The authors declare that they have no competing financial interests.

Correspondence and requests for materials should be addressed to P.A.B. (e-mail: paul.bruhwiler@fysik.uu.se).

Ecosystem carbon loss with woody plant invasion of grasslands

Robert B. Jackson*, Jay L. Banner†, Esteban G. Jobbágy*, William T. Pockman*‡ & Diana H. Wall§

** Department of Biology and Nicholas School of the Environment and Earth Sciences, Duke University, Durham, North Carolina 27708-0340, USA*
† Department of Geological Sciences, University of Texas at Austin, Austin, Texas 78712, USA
§ Natural Resource Ecology Laboratory, Colorado State University, Fort Collins, Colorado 80523, USA

The invasion of woody vegetation into deserts, grasslands and savannas is generally thought to lead to an increase in the amount of carbon stored in those ecosystems. For this reason, shrub and forest expansion (for example, into grasslands) is also suggested to be a substantial, if uncertain, component of the terrestrial carbon sink[1–14]. Here we investigate woody plant invasion along a precipitation gradient (200 to 1,100 mm yr^{-1}) by comparing carbon and nitrogen budgets and soil $\delta^{13}C$ profiles between six pairs of adjacent grasslands, in which one of each pair was invaded by woody species 30 to 100 years ago. We found a clear negative relationship between precipitation and changes in soil organic carbon and nitrogen content when grasslands were invaded by woody vegetation, with drier sites gaining, and wetter sites losing, soil organic carbon. Losses of soil organic carbon at the wetter sites were substantial enough to offset increases in plant biomass carbon, suggesting that current land-based assessments may overestimate carbon sinks. Assessments relying on carbon stored from woody plant invasions to balance emissions may therefore be incorrect.

One-third to one-half of the Earth's land surface has been transformed by human action[2,4]. Many continuing transformations exchange woody and herbaceous plants[15–18], including deforestation, desertification, and woody plant invasion (the expansion of woody species into grasslands and savannas). Shifting dominance among herbaceous and woody vegetation alters primary production, plant allocation, rooting depth and soil faunal communities, potentially metres underground[15,18], in turn affecting nutrient cycling and carbon storage[19,20]. The two carbon pools most likely to change are woody plant biomass and soil organic matter, the dominant pool of carbon and nitrogen in grasslands[10,20–23]. New woody biomass stores carbon in amounts that depend on the age, productivity and density of the stand. Changes in soil organic carbon (SOC) over the entire rooting zone are much harder to predict, and have the potential to enhance or offset biomass carbon gains, complicating projections of ecosystem carbon storage.

On the basis of a global analysis of more than 2,700 SOC profiles[20], we examined where increased biomass C in woody plants might be offset by SOC losses (see Methods). Across the global data set, the slope of the relationship between SOC and precipitation was 2.6 times higher for grassland vegetation than for shrublands/woodlands ($P = 0.001$; see Supplementary Information). Whereas grassland SOC was statistically indistinguishable from values for woody plants at 200 mm mean annual precipitation, woodlands had 43% less total SOC than grasslands at 1,000 mm ($P < 0.01$). Although suggestive, this analysis lacked a direct test of vegetation change independent of other covarying factors, including soil properties. So we also examined the direct effect of vegetation change at six paired grassland and invaded woody sites along a

‡ Present address: Department of Biology, University of New Mexico, Albuquerque, New Mexico 87131-1091, USA.

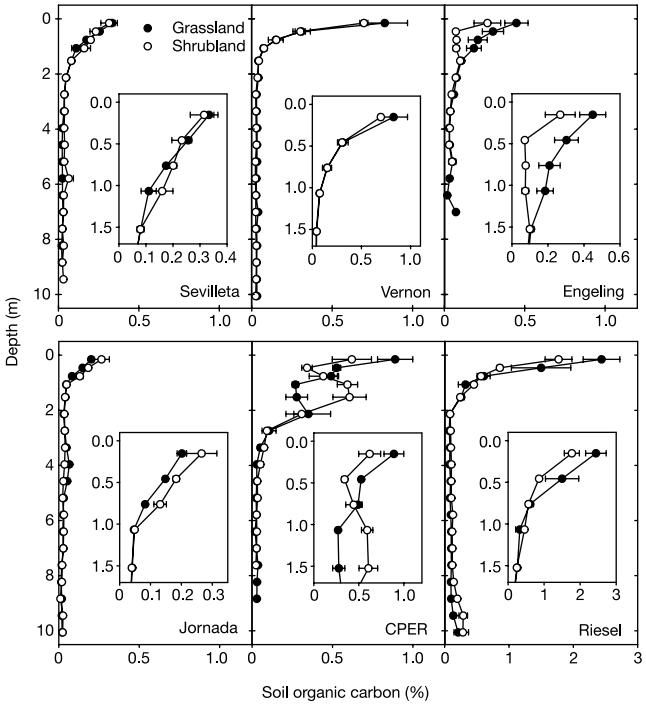

Figure 1 Concentrations of total soil organic carbon with depth. Data are shown for six paired grassland (filled circles) and woody sites (open circles) along the precipitation gradient (mean ± s.e.; $n = 3$–8). The panels are arranged from driest on the left to wettest on the right (analogous to the west-to-east precipitation gradient). The insets present the data for the top 1.5 m of soil at higher resolution. See Methods and Table 1 for additional information.

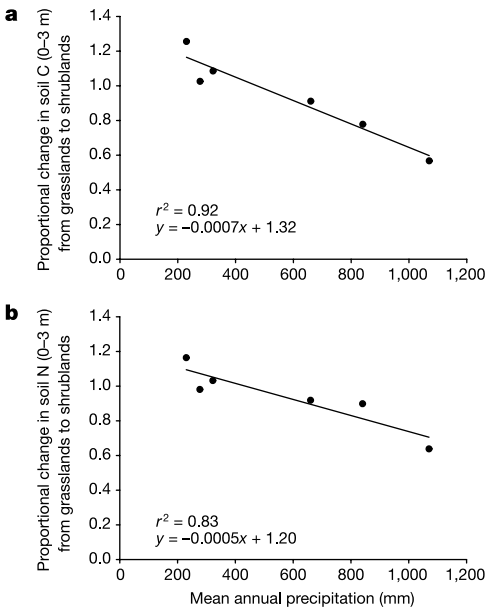

Figure 2 The proportional change in total soil organic carbon (**a**) and nitrogen (**b**) to 3 m depth with woody plant invasion of native grasslands. Values >1 are for those sites that gained soil organic carbon (SOC) and soil organic nitrogen (SON) after woody plant invasion, and values <1 denote a loss. See Table 1 for the key to the sites, mean annual precipitation, and the woody species.

rainfall gradient in the southwestern USA (see Methods), testing relationships of biomass C gains and SOC losses for such common native woody invaders as *Prosopis* (mesquite), *Larrea* (creosote) and *Juniperus* (juniper) spp. (Table 1).

Along the precipitation gradient, woody plant invasion increased contents of SOC and soil organic nitrogen (SON) at the drier sites, and decreased them at the wetter sites (Fig. 1, Table 2). Jornada gained approximately one-quarter of total SOC after woody plant invasion (9 Mg ha^{-1}), but the two wettest sites lost one-fifth to almost one-half of total SOC (Table 2). Differential changes along the gradient resulted in a clear linear decline for the amounts of SOC and SON in the top 3 m of soil after conversion to woody plants (Fig. 2; $P \leq 0.01$ for both). Absolute changes in SOC and SON were also greater at the wetter sites; whereas none of the three desert sites gained more than 13 Mg ha^{-1} of SOC, the three wetter sites lost about 8, 32 and 61 Mg ha^{-1} (or about 0.25–0.8 Mg C ha^{-1} yr^{-1}; Tables 1 and 2). The close agreement between the loss of SOC at Engeling (a 44% reduction in SOC at 1,070 mm precipitation) and the database prediction (43% reduction in SOC at 1,000 mm precipitation) is notable.

SOC and SON were also more deeply distributed at the woody sites. Compared to the top metre of soil, there was 60% as much SOC at 1 to 3 m depth in the woodlands but only 40% in the grasslands (Table 2). Riesel lost 65 Mg C ha^{-1} and 3.9 Mg N ha^{-1} with woody plant invasion in the top metre of soil, but gained C and N slightly from 1 to 3 m depth; the CPER shrubland had 50% more SOC and SON between 1 and 3 m, but one-fifth less from 0 to 1 m compared to the grassland (Table 2).

Total ecosystem C stocks shifted both in size and in distribution above and below ground. Plant biomass C increased with woody plant invasion at all sites (0.3–44 Mg C ha^{-1}), but the changes were smaller than for SOC at five of them (Table 2). The most notable shift in C from below-ground to above-ground pools was at the wettest site, Engeling, where 44 Mg C ha^{-1} of new plant C offset the SOC loss of 32 Mg ha^{-1} in the ~40 years since juniper invasion. Such shifts make C stocks more vulnerable to loss from fire, biomass harvesting and other disturbances. The biggest total change in C storage was for the Riesel tallgrass prairie site. There, a slight increase in plant biomass C was an order of magnitude smaller than SOC losses, resulting in a net loss of 56 Mg C ha^{-1} (Table 2). Total changes in ecosystem C pools at the other sites were more modest (−3 to 13 Mg C ha^{-1}; Table 2).

Table 1 **Descriptions and comparisons of the six study sites**

Site	Location (°N, °W)	MAP* (mm)	Age† (yr)	Mean 95% rooting depth‡ (m)	Nematodes max. depth‡§ (m)	Mean depth of Sr uptake‡‖ (m)
Jornada, NM	32.5, 106.8	230	>50	1.7, 5.4	1.8, 0.6	2.8, >3.0
Sevilleta, NM	34.3, 106.7	277	40	0.6, 2.0	0.6, 7.4	1.9, <1.2
CPER, CO	40.9, 104.7	322	>50	0.9, 4.0	2.5, 3.7	0.2, 1.4
Vernon, TX	33.9, 99.4	660	30	0.9, 5.8	4.3, 4.3	0.2, 0.1
Riesel, TX	31.5, 96.9	840	75–100	0.8, 2.8	1.8, 6.8	0.1, 2.4
Engeling, TX	31.9, 95.9	1,070	40	3.3, 2.5	1.2, 1.2	NA

*Mean annual precipitation.
†Approximate age of the woody stands at each site.
‡Values given are for grasslands, woodlands.
§Maximum depth of soil nematode occurrence at each site.
‖Integrated depth of soil Sr uptake ($^{87}Sr/^{86}Sr$ ratios; see Methods and Supplementary Information). NA, not available.

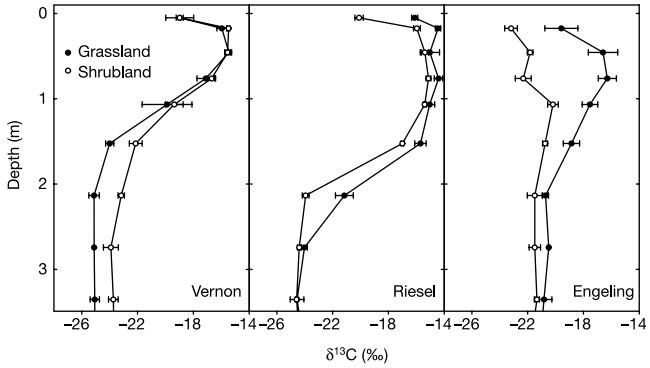

Figure 3 $\delta^{13}C$ values of soil organic carbon for the three wettest sites—Vernon, Riesel and Engeling. See Methods and Table 1 for additional information. Reference standard is Pee Dee Belemnite (V-PDB).

Examining in more detail the wetter sites where the greatest shifts occurred, we found that changes in C isotope signatures (Fig. 3) and N concentrations (see Supplementary Information) mirrored those for SOC pools (Fig. 1). The $\delta^{13}C$ data, reflecting differences in the photosynthetic pathway of C fixation for C_3 woody species and C_4 grasses[17], show that the differences observed for grasslands and shrublands were not simply the result of losses of original SOC: new SOC was clearly incorporated into the system (Fig. 3). Using the assumptions of a two-layer mixing model (see Methods), ~57% of the SOC in the Engeling woodland came from the juniper trees in the ~40 years since invasion, with 43% of SOC in the woodland attributable to the original grassland SOC. At Riesel, about 20% of the SOC in the mesquite stand was attributable to the trees (Fig. 3).

Rooting depths, nematode distributions, and the integrated depth of soil cation uptake all changed substantially with woody plant invasion (Table 1). Mean 95% rooting depths were >2 m deeper on average for the woody vegetation at the six paired sites ($P \leq 0.01$), with increases of 3 to 4 m at Jornada, CPER and Vernon. Only Engeling showed no evidence of increased rooting depths with invasion. We also examined the representative soil biota most closely dependent on roots as indicator taxa—parasitic nematodes and nematodes feeding on rhizosphere bacteria and fungi. Their maximum depth of occurrence increased from 2.1 m on average in grasslands to 4.0 m for the woody sites (Table 1), and the composition of the nematode food web at this depth was markedly reduced from five trophic groups to two (bacterial- and root-feeding nematodes). Invaded woody sites also had lower species richness, 26 compared with 31 taxa, with the difference primarily due to the loss of root-feeding species. These responses of the nematode community to plant invasions are similar to changes in the soil food web with other disturbances, such as conversion to agriculture, that can alter rates of herbivory and decomposition[24].

We estimated the integrated depth of nutrient uptake using natural isotopes of Sr, an element geochemically similar to Ca (ref. 25) that is taken up by the same transporters in plants and undergoes negligible biological fractionation. Sr isotope ratios of the grasses at the wetter sites closely matched soil signatures in the shallowest layers, but at the two driest grasslands the integrated depth of uptake was a surprising 2 to 3 m (Table 1; see Supplementary Information). Just as importantly, woody plant invasion increased the depth of Sr uptake at three sites by as much as 2 m (Table 1).

Our global database analysis and fieldwork both suggest an important role for precipitation in understanding the consequences of desertification and woody plant invasions. Nonetheless, the database also showed significant unexplained variation in SOC storage. Many biotic and abiotic factors determine SOC storage[13,20,26,27]. Soil factors can influence SOC concentrations and the occurrence of woody encroachment[28]. In a south Texas savanna, for example, soil texture and the presence of an argillic horizon strongly influence where *Prosopis* establishes[28]. The condition and productivity of grasslands before invasion are also important. Relatively wet grasslands are often highly productive, allocating a large proportion of C below ground, and have high SOC concentrations[13,20,23]. An analysis of 115 studies concluded that sites originally dominated by woodlands showed the greatest potential of all biomes for storing C as managed pastures[29], in part because of high grassland productivity and below-ground allocation there. A similar meta-analysis of land conversion from managed pastures to plantations in New Zealand also documented soil carbon losses[13]. Historical factors and disturbance, including erosion and fire frequency, play additional roles[26,27]. Modelling simulations of the *Prosopis* savanna mentioned above[28] suggest that one-fifth of SOC could be lost with grazing before woody plant invasion. Of these many potential factors, our experimental design isolated the role of vegetation change for C storage and ecosystem functioning in the absence of background differences in soils.

Potential C storage in plant biomass is common as woody plants invade grasslands. Nonetheless, current uncertainties for net changes in C stocks are large, as are the uncertainties in regional extrapolations of woody plant invasions[11,12]. Recent analyses have nevertheless concluded that the US carbon budget is approximately balanced[11]. Our data suggest that this conclusion may be premature.

Table 2 **Soil organic C and N to 3 m depth and total changes in C pools after woody plant invasion**

		Soil organic carbon (Mg ha^{-1})			Soil organic nitrogen (Mg ha^{-1})			Net Δ C (Mg ha^{-1})	
Site	Depth	Grassland	Shrub- or woodland	Change (%)	Grassland	Shrub- or woodland	Change (%)		
Jornada	0–1 m	24.6	32.9	+33%	3.2	3.8	+21%	Soil	8.7
	1–3 m	9.2	9.6	+5%	1.3	1.3	+6%	Plant	1.4
	0–3 m*	33.8	42.5	+26%	4.4	5.2	+16%	Total	10.1
Sevilleta	0–1 m	38.0	38.0	0%	4.8	4.7	−4%	Soil	1.4
	1–3 m	14.6	16.0	+10%	1.5	1.5	+4%	Plant	0.4
	0–3 m*	52.6	54.0	+3%	6.3	6.2	−2%	Total	1.8
CPER	0–1 m	89.3	70.8	−21%	10.5	7.6	−27%	Soil	12.8
	1–3 m	60.8	92.1	+52%	6.2	9.6	+55%	Plant	0.3
	0–3 m*	150	163	+9%	16.7	17.3	+3%	Total	13.1
Vernon	0–1 m	72.4	65.0	−10%	9.4	8.4	−11%	Soil	−7.6
	1–3 m	13.7	13.5	−1%	5.4	5.2	−4%	Plant	4.7
	0–3 m*	86.1	78.5	−9%	14.8	13.6	−8%	Total	−2.9
Riesel	0–1 m	229	164	−28%	20.2	16.4	−19%	Soil	−61.4
	1–3 m	48.4	51.9	+ 7%	6.2	7.4	+19%	Plant	5.3
	0–3 m*	278	216	−22%	26.4	23.7	−10%	Total	−56.1
Engeling	0–1 m	47.9	20.7	−57%	4.0	1.6	−59%	Soil	−32.2
	1–3 m	26.0	21.0	−20%	2.9	2.8	−5%	Plant	44.4
	0–3 m*	73.9	41.7	−44%	6.9	4.4	−37%	Total	12.2

*Values of SOC and SON for 0–3 m depth are the sum of the respective values at 0–1 and 1–3 m depth.

On the basis of the database analysis presented here and on the observed losses of SOC in the wetter grasslands, further field studies and modelling integration will be needed to evaluate the net effects of woody plant invasions for the C cycle and to close the C budget. □

Methods

Database analysis

The global analysis of the variation of SOC with precipitation was derived from the National Soil Characterization Database of the USDA and the World Inventory of Soil Emission Potential Database of the International Soil Reference and Information Centre (see ref. 20). Mean annual precipitation for each location was obtained with a resolution of $0.5° \times 0.5°$ from the International Institute for Applied Systems Analysis. The analysis considered soils to 1-m depth (insufficient data existed for deeper depths) at all sites with <1,000 mm mean annual precipitation except Histosols (for example, organic soils in bogs and marshes) and Udi/Ustipsamments (dune soils). Herbaceous-dominated communities excluding riparian meadows and tundra were considered grasslands, and woodland, brush, chaparral, scrub, shrub steppe, or shrub desert communities were considered woody sites. The final regression statistics for SOC ($kg\,C\,m^{-2}$) with mean annual precipitation (mm) were as follows. Grasslands: y intercept, 3.253; slope, 0.0152; $r^2 = 0.33$; $P < 0.001$; $n = 75$. Woody vegetation: y intercept, 4.629; slope, 0.00595; $r^2 = 0.12$; $P < 0.001$; $n = 167$ (see Supplementary Information). Because many factors change or are correlated with rainfall, this analysis merely suggested a strong interaction with precipitation.

Experimental design and soil sampling

Field measurements were made in adjacent communities at the six locations in Table 1. The 200,000-ha Waggoner ranch is the long-term research site for the Vernon, Texas, Research Station of Texas A&M University. The Riesel site maintained by the USDA/Agriculture Research Service, and the Gus Engeling Wildlife Management Area operated by the Texas Parks and Wildlife Department, have been maintained by these agencies for >50 years. The other sites are part of the international Long Term Ecological Research (LTER) network. On the basis of aerial photographs and additional records, the youngest age of the woody stands was 30 to 40 years (Sevilleta, Vernon and Engeling). The dominant grasses at each site were *Bouteloua eriopoda* at Jornada and Sevilleta, *Bouteloua gracilis* at CPER, *Stipa* sp. at Vernon, *Schizachyrium scoparium* at Riesel, and *Andropogon* sp. at Engeling.

Each site contained adjacent grassland and shrub/woodland communities where management practices have contributed to woody plant expansion into native grasslands on one side of a fence. The goal of this paired experimental design was to compare the effects of herbaceous and woody communities without initial differences in soil properties. The one site where initial differences may have existed was the Shortgrass Steppe LTER (CPER), as revealed by the background soil profiles of Sr isotopes (see Supplementary Information).

In each of the two communities per site, four to nine 6-cm-diameter cores were taken with an environmental drilling rig to 10-m depth. The cores were extracted between May and October 1997 (the approximate time of peak biomass at each site) in 61-cm increments, and were subsequently air-dried and passed through a 2-mm sieve, where roots were extracted and quantified. To remove soil inorganic C (present in a subset of samples at all sites except Engeling), soil samples were treated with 1 N H_2SO_4/5% $FeSO_4$ and double-checked for complete inorganic C removal. Total SOC and N were measured as in ref. 30 using a CE Instruments NC 2100 elemental analyser (ThermoQuest Italia), with a subset of measurements confirmed independently. The $\delta^{13}C$ SOC measurements were run on a Finnigan MAT DeltaPlusXL mass spectrometer at Duke University. The grasslands generally had a mixture of C_3 and C_4 species, so the grassland $\delta^{13}C$ signatures were used as one end of a two-layer mixing model for the approximate calculations of C derived from the woody plants after invasion. The shrubs were estimated to have a $\delta^{13}C$ signature of −26‰, typical for C_3 plants. Total SOC and N concentrations were converted to ecosystem estimates using the bulk density at each depth and correcting for the presence of any rocks (>2 mm) (see Supplementary Information). To help address any spatial heterogeneity and to supplement data from the deep cores, 25-cm-diameter soil pits were dug to 50-cm depth randomly in each community ($n \geq 4$ per community). The soil subsamples for nematodes were sent immediately to Colorado State University for analysis[24]. Sr isotope analyses of soil and plant material were determined at the University of Texas at Austin using a Finnigan-MAT 261 thermal ionization mass spectrometer in automated, dynamic multi-collection mode (see Supplementary Information).

Proportional changes in total SOC and SON to 3-m depth with woody plant invasion (Fig. 2) were analysed by regression ($n = 6$), using precipitation as the dependent variable. Other statistical determinations were calculated by paired t-test.

Plant biomass C

Herbaceous biomass in grassland communities was estimated by harvesting all material in random 0.5 m × 0.5 m plots ($n \geq 4$ per community). Live and dead standing biomass were separated, oven dried, weighed, and converted to biomass C. At the drier end of the precipitation gradient, significant herbaceous biomass also occurred in the shrubland communities. There, four under-canopy and four open positions were randomly selected for 0.5 m × 0.5 m herbaceous harvest plots. The proportions of under-canopy and open positions were estimated using three randomly located 60-m Canfield transects per community, with mean herbaceous biomass adjusted by the proportional cover of each position. For woody plant biomass, the density of plants was determined in each of three random 10 m × 20 m plots per community, with plant biomass harvested in each plot. Wood and leaf samples were separated, oven dried, weighed, and converted from total biomass to biomass C. Fine root biomass estimates were obtained from the soil cores after sieving, drying and ashing the root samples. Large woody roots (>1 cm diameter) were the only C pool not quantified in this study.

Received 14 January; accepted 14 June 2002; doi:10.1038/nature00910.

1. Schlesinger, W. H. *et al.* Biological feedbacks in global desertification. *Science* **247,** 1043–1048 (1990).
2. Vitousek, P. M., Mooney, H. A., Lubchenco, J. & Melillo, J. M. Human domination of Earth's ecosystems. *Science* **277,** 494–499 (1997).
3. Schimel, D. S. *et al.* Recent patterns and mechanisms of carbon exchange by terrestrial ecosystems. *Nature* **414,** 169–172 (2001).
4. Turner, B. L. II *et al.* (eds) in *The Earth as Transformed by Human Action* (Cambridge Univ. Press, Cambridge, 1990).
5. Tucker, C. J., Dregne, H. E. & Newcomb, W. W. Expansion and contraction of the Sahara Desert from 1980 to 1990. *Science* **253,** 299–301 (1991).
6. Scholes, R. J. & Archer, S. R. Tree-grass interactions in savannas. *Annu. Rev. Ecol. Syst.* **28,** 517–544 (1997).
7. Brown, J. H., Valone, T. J. & Curtin, C. G. Reorganization of an arid ecosystem in response to recent climate change. *Proc. Natl Acad. Sci. USA* **94,** 9729–9733 (1997).
8. Allen, C. D. & Breshears, D. D. Drought-induced shift of a forest-woodland ecotone: rapid landscape response to climate variation. *Proc. Natl Acad. Sci. USA* **95,** 14839–14842 (1998).
9. Casper, B. B. & Jackson, R. B. Plant competition underground. *Annu. Rev. Ecol. Syst.* **28,** 545–570 (1997).
10. Amundson, R. The carbon budget in soils. *Annu. Rev. Earth Planet. Sci.* **29,** 535–562 (2001).
11. Pacala, S. W. *et al.* Consistent land- and atmosphere-based U.S. carbon sink estimates. *Science* **292,** 2316–2320 (2001).
12. Houghton, R. A., Hackler, J. L. & Lawrence, K. T. The U. S. carbon budget: contributions from land-use change. *Science* **285,** 574–578 (1999).
13. Guo, L. B. & Gifford, R. M. Soil carbon stocks and land use change: a meta analysis. *Glob. Change Biol.* **8,** 345–360 (2002).
14. Fang, J. Y., Chen, A. P., Peng, C. H., Zhao, S. Q. & Longjun, C. Changes in forest biomass carbon storage in China between 1949 and 1998. *Science* **292,** 2320–2322 (2001).
15. Nepstad, D. C. *et al.* The role of deep roots in the hydrological and carbon cycles of Amazonian forests and pastures. *Nature* **372,** 666–669 (1994).
16. Van Auken, O. W. Shrub invasions of North American semiarid grasslands. *Annu. Rev. Ecol. Syst.* **31,** 197–215 (2000).
17. Boutton, T. W. *et al.* Delta C-13 values of soil organic carbon and their use in documenting vegetation change in a subtropical savanna ecosystem. *Geoderma* **82,** 5–41 (1998).
18. Jackson, R. B. *et al.* Belowground consequences of vegetation change and their treatment in models. *Ecol. Appl.* **10,** 470–483 (2000).
19. Trumbore, S. E. Potential responses of soil organic carbon to global environmental change. *Proc. Natl Acad. Sci. USA* **94,** 8284–8291 (1997).
20. Jobbágy, E. G. & Jackson, R. B. The vertical distribution of soil organic carbon and its relation to climate and vegetation. *Ecol. Appl.* **10,** 423–436 (2000).
21. Post, W. M., Emanuel, W. R., Zinke, P. J. & Stangenberger, A. G. Soil carbon pools and world life zones. *Nature* **298,** 156–159 (1982).
22. Batjes, N. H. Total carbon and nitrogen in the soils of the world. *Eur. J. Soil Sci.* **47,** 151–163 (1996).
23. Neill, C. & Davidson, E. A. in *Global Climate Change and Tropical Ecosystems* (eds Lal, R., Kimble, J. M. & Stewart, B. A.) 197–211 (CRC, Boca Raton, 2000).
24. Wall, D. H., Adams, G. A. & Parsons, A. N. in *Global Biodiversity in a Changing Environment* (eds Chapin, F. S., Sala, O. E. & Huber-Sannwald, E.) 47–82 (Springer, New York, 2001).
25. Vitousek, P. M., Kennedy, M. J., Derry, L. A. & Chadwick, O. A. Weathering versus atmospheric sources of strontium in ecosystems on young volcanic soils. *Oecologia* **121,** 255–259 (1999).
26. Burke, I. C. *et al.* Texture, climate, and cultivation effects on soil organic matter content in U.S. grassland soils. *Soil Sci. Soc. Am. J.* **53,** 800–805 (1989).
27. Tilman, D. *et al.* Fire suppression and ecosystem carbon storage. *Ecology* **81,** 2680–2685 (2000).
28. Archer, S., Boutton, T. W. & Hibbard, K. A. in *Global Biogeochemical Cycles in the Climate System* (eds Schulze, E.-D. *et al.*) 115–137 (Academic, San Diego, 2001).
29. Conant, R. T., Paustian, K. & Elliott, E. T. Grassland management and conversion to grassland: effects on soil carbon. *Ecol. Appl.* **11,** 343–355 (2001).
30. Gill, R. A. *et al.* Nonlinear grassland responses to past and future atmospheric CO_2. *Nature* **417,** 279–282 (2002).

Supplementary Information accompanies the paper on *Nature*'s website (http://www.nature.com/nature).

Acknowledgements

We thank W. Cook, L. Giles, J. Karr, L. Mack, A. Parsons and S. Rainey for laboratory analyses, and W. H. Schlesinger, A. T. Austin, O. E. Sala and E. A. Davidson for manuscript suggestions. We also thank R. J. Ansley, H. W. Polley and many others who helped us locate sites and provide their history. This work was supported by the US National Science Foundation, NIGEC/DOE, the Inter-American Institute for Global Change Research, the Andrew W. Mellon Foundation, and the Geology Foundation of the University of Texas at Austin. This paper is a contribution to the Global Change and Terrestrial Ecosystems core project of the International Geosphere Biosphere Programme.

Competing interests statement

The authors declare that they have no competing financial interests.

Correspondence and requests for materials should be addressed to R.B.J. (e-mail: jackson@duke.edu).

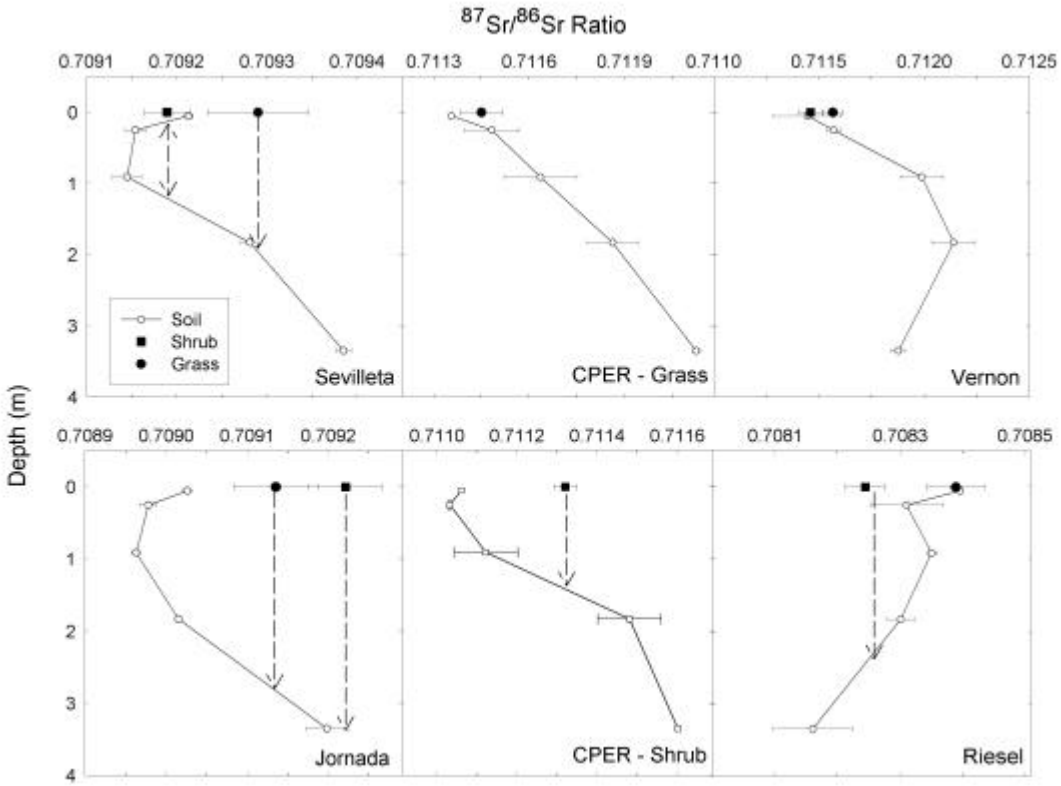

Supplementary Figure 1. $^{87}Sr/^{86}Sr$ values for soil (open circles) and bulk leaves of grasses (filled circles) and woody species (filled squares) (mean ± s.e.; n=2 to 5; analytical uncertainty ± 0.000015). The arrows show the points at which the Sr ratios in vegetation match the values for the soil profiles; actual Sr uptake likely comes from depths both below and above these points in a combination that provides the observed plant ratios. The data for grasses and shrubs at the Shortgrass Steppe LTER (CPER) are presented in two panels because of differences in background soil Sr signatures.

Methods and Description. Plant samples were ground, ashed at 500 to 800°C, and dissolved in concentrated HNO_3. Exchangeable soil Sr was extracted by leaching ≈4 g of soil for 20 min. with 10 ml of 0.5M ammonium acetate adjusted to pH 8 (Ref 1). Plant and exchangeable soil Sr were purified using EIChrome Sr Spec resin, dissolved, and evaporated onto either zone-refined Re filaments with a H_3PO_4 + Ta_2O_5 slurry loading medium (plant Sr) or Ta filaments with H_3PO_4 (soil Sr).

Sr isotope analyses at the University of Texas at Austin used a Finnigan-MAT 261 thermal ionization mass spectrometer in automated, dynamic multi-collection mode. $^{87}Sr/^{86}Sr$ values were normalized for fractionation on-line to 0.1194 using an exponential fractionation law, and were corrected offline for fractionation based on an empirical relationship between instrument fractionation and $^{87}Sr/^{86}Sr$ value. Each $^{87}Sr/^{86}Sr$ value represented the mean of 60 to 105 individual ratios (4 to 7 blocks of 15 scans per block). The mean value for the NBS-SRM 987 standard over the course of this study was 0.710271 ± 0.000015 (2σ external, n = 26). All sample blanks contained <85 pg Sr compared to >200 ng Sr in samples analyzed.

1. Suarez, D. L., Beryllium, Magnesium, Calcium, Strontium, and Barium, in: Methods of Soil Analysis. Part 3. Chemical Methods - SSSA Book Series no. 5, Soil Science Society of America and American Society of Agronomy, Madison, WI (1996).

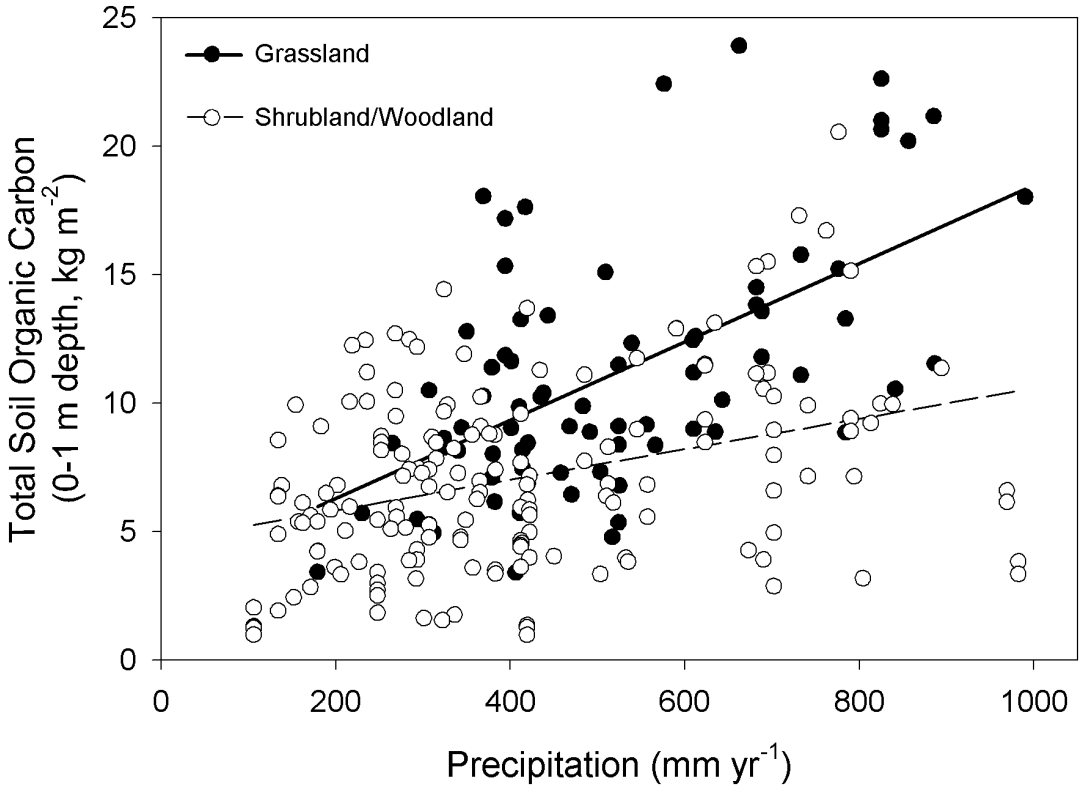

Legend for the database figure: An analysis of soil organic carbon (kg m^{-2}) versus mean annual precipitation (mm) for the top meter of soil. The data are derived from the National Soil Characterization Database of the U.S. Department of Agriculture and the World Inventory of Soil Emission Potential Database of the International Soil Reference and Information Centre. See Methods for additional information and for a description of the regression lines.

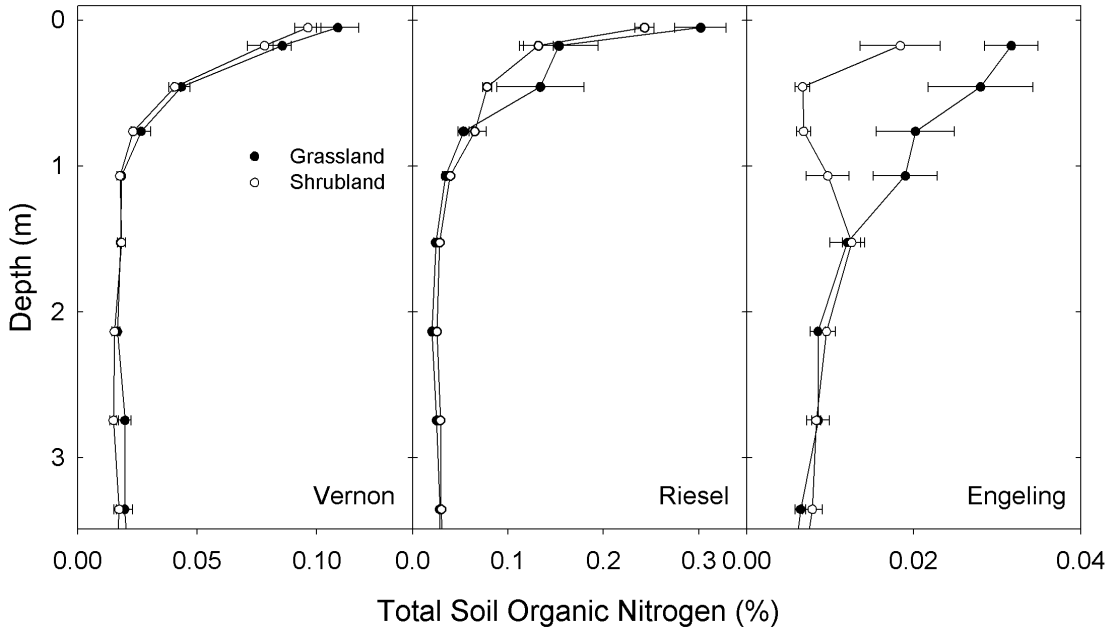

Legend for the soil organic nitrogen figure: Total soil organic nitrogen (%) with depth (m) for three paired grassland (filled circles) and woody sites (open circles) along the precipitation gradient (mean ± s.e.; n=4 to 8). The three wettest sites are arranged from driest on the left to wettest on the right (analogous to the west-to-east precipitation gradient). See Methods and Table 1 for additional information.

Supplemental Table . Stone content (>2 mm, % Vol.) and soil bulk density (g cm^{-3}) to 3 m depth (mean and standard deviation)

Site	Depth	Stone Content (% by volume)	Soil Bulk Density (g cm^{-3})
Jornada	0-1 m	0.06 (0.08)	1.8 (0.18)
	1-2 m	0.60 (1.6)	1.6 (0.16)
	2-3 m	8.6 (9.2)	1.9 (0.18)
Sevilleta	0-1 m	7.9 (3.1)	1.7 (0.12)
	1-2 m	14.2(4.4)	1.6 (0.15)
	2-3 m	12.5 (7.6)	1.5 (0.33)
CPER	0-1 m	0.43 (0.87)	1.5 (0.14)
	1-2 m	1.6 (3.1)	1.3 (0.20)
	2-3 m	3.4 (5.0)	1.5 (0.22)
Vernon	0-1 m	0	1.8 (0.42)
	1-2 m	0	2.1 (0.09)
	2-3 m	0	2.1 (0.23)
Riesel	0-1 m	0	1.6 (0.12)
	1-2 m	0	1.8 (0.12)
	2-3 m	0	1.7 (0.06)
Engeling	0-1 m	0.12 (0.20)	1.6 (0.15)
	1-2 m	0.20 (0.28)	1.8 (0.17)
	2-3 m	8.3 (7.7)	1.8 (0.22)